Numerical simulations of solvation dynamics in electrolyte solutions

Eyal Neria and Abraham Nitzan
School of Chemistry, The Sackler Faculty of Science, Tel Aviv University, Tel Aviv 69978, Israel

(Received 8 September 1993; accepted 19 November 1993)

Recent experimental studies of solvation dynamics in electrolyte solutions indicate the existence of a slow dynamical component associated with the salt ions. This contribution cannot be accounted for by the Debye–Falkenhagen theory of ionic atmosphere response. Molecular dynamics simulations of solvation dynamics in a simple model (Stockmayer solvent containing spherical ions) of electrolyte solution are presented. The simulations confirm the interpretation that the slow dynamical component is primarily an outcome of ion exchange between the first solvation shell about the solute and the solution bulk. The simulations also indicate the highly correlated motion between the salt ions and the solvent molecules.

I. INTRODUCTION

Recent experimental, numerical, and theoretical studies of solvation dynamics following solute charge redistribution in pure polar solvents[1–3] have led to several studies of similar processes in electrolyte solutions.[4–6] These works have revealed the existence of a new relaxation mode associated with the rearrangement of the ionic atmosphere around the newly formed charge distribution. This paper describes the results of numerical simulation studies of solvation dynamics in such systems.

Numerical simulations of solvation dynamics in several models of simple polar solvents[3] have yielded a uniform picture: solvent relaxation following a sudden creation (or change) of a charge distribution is essentially bimodal: The solvation function

$$S(t)=\frac{E(t)-E(\infty)}{E(0)-E(\infty)}, \tag{1}$$

in which $E(t)$ is the solvation energy at time t (assumed to be proportional to the experimentally observed shift in the fluorescence spectrum) can be fit to a superposition of a Gaussian and an exponential function,

$$S(t)=A_g e^{-(t/\tau_g)^2}+A_e e^{-t/\tau_e}. \tag{2}$$

The Gaussian component corresponds to an ultrafast underdamped solvent relaxation which accounts for 60%–80% of the solvation energy. The residual, exponential component is related to the "conventional" diffusive relaxation which had been assumed to dominate solvation dynamics in earlier studies. The predominant role played by the inertial Gaussian component has been recently demonstrated experimentally[7] and analyzed theoretically.[8]

Recent experimental studies by Huppert and coworkers[4] and by Chapman and Maroncelli[5] have revealed several phenomena associated with salt effects on solvation and solvation dynamics. These experiments involve a chromophore "probe" dissolved in one of several dielectric solvents representing a range of dielectric permeabilities (ε_s, the solvent static dielectric coefficient ranging from 6 for ethyl acetate to 111 for formamide). Several added salts were studied with concentrations in the range 10^{-3}–$3.0M$. The main findings of these studies are:

(1) The addition of salt causes a red shift in the steady-state absorption and emission spectra of the probe solute, above the shift induced by the pure solvent. This ion induced frequency shift is of the order of several hundred cm^{-1} for a $1M$ salt concentration. The magnitude of these shifts decreases when the solvent polarity increases. For formamide ($\varepsilon_s=111$) and water ($\varepsilon_s=80$) these shifts are almost unobservable.

(2) The magnitudes of the observed shifts, as functions of the type of salt added, are primarily functions of the cation type, and correlate approximately linearly with the cation's charge-to-radius ratio.

(3) The relaxation which follows the probe's optical excitation (associated with a sudden rearrangement of its charge distribution) can be separated into its solvent and electrolyte components. The solvent response is faster by one to three orders of magnitude than the ionic relaxation, and could not usually be resolved in the given experimental setups. The additional relaxation associated with the added electrolyte occurs on a time scale of up to several nanoseconds. The added salt affect the spectral width far less than the spectral peak position.

(4) The ionic relaxation is generally nonexponential, the average relaxation time depends linearly, at constant temperature and for electrolyte concentration $\leqslant 1M$, on η/c where c is the electrolyte concentration and η is the solvent bulk viscosity (at the given electrolyte concentration). The temperature dependence of the dynamics indicate activation energies substantially larger than those inferred from the solvent viscosity.

(5) The ionic relaxation time depends approximately linearly on the solvent polarity expressed by its static dielectric response ε_s. A better correlation is found with E_T^N, the normalized $E_T(30)$ polarity scale introduced by Reichardt.[9] The relaxation time also depends on the nature of the salt, in particular of the cation involved: It increases with the charge-to-radius ratio of the cation.

(6) The kinetics of the solvation process in ionic solutions is not homogeneous, and depend on the excitation frequency employed.

It is important to emphasize[5] that even though this summary of results seems to imply that the solvent and electrolyte contributions to the spectral shift and to the

 0021-9606/94/100(5)/3855/14/$6.00

relaxation times are separable and additive, no true separability exists. In particular, ion motions by necessity imply additional solvent rearrangement. However, the time scale separation imply that the fast solvent adiabatically follows the ions' motion. This issue is examined in the simulation results described below. In addition, in the few cases where the fast solvent dynamics could be resolved (e.g., in propanol[5]) it was observed to scale with the viscosity which in turn depends on the salt concentration.[10]

On the theoretical side, it is natural to consider first the energetics of solvation in ionic solutions as implied by the Debye–Hückel (DH) theory,[11] and the corresponding dynamics of the ion atmosphere relaxation that was studied by Debye and Falkenhagen (DF)[12] under the same equilibrium assumptions as the DH theory, and with the additional assumption that relaxation takes place by diffusive motion. Van der Zwan and Hynes[6] have recently studied the influence of ion atmosphere dynamics on a model dipolar isomerization reaction in an electrolyte solution. They have shown, within the framework of the DH and DF theories (extended to the case of a central dipole instead of a central ion), that the ion atmosphere friction can sometimes have a substantial effect in reducing the reaction rate below the equilibrium solvation transition state theory. Here we limit ourselves to the contribution of the ionic atmosphere to the solvation energy and to the relaxation dynamics of this atmosphere. The former is given, for a central ion of charge Q and radius a, by

$$W_s=-\frac{Q^2}{2a}\left(\frac{\kappa a}{\varepsilon_s(1+\kappa a)}+\left[1-\frac{1}{\varepsilon_s}\right]\right), \tag{3}$$

where

$$\kappa=\left[\frac{4\pi\Sigma_j q_j^2 c_j}{\varepsilon_s k_B T}\right]^{1/2} \tag{4}$$

is the Debye length. The sum in Eq. (4) goes over all ion types in the solution, with charges q_j and concentrations c_j. In Eq. (3) the term in the inner square brackets accounts for the solvent contribution to the solvation energy. The other term, approximately equal (for $\kappa a \ll 1$) to

$$W_s(\text{ion}) \cong Q^2\kappa/(2\varepsilon_s), \tag{5}$$

is the electrolyte contribution. Note that the theory is valid only if $\kappa a \ll 1$ and $q_i q_j/(\varepsilon_s r_s k_B T) \ll 1$, where $r_s=[3/(4\pi c)]^{1/3}$ is the average distance between ions ($c=\Sigma_j c_j$). It is immediately realized that for $c \geqslant 0.1M$ these conditions are not satisfied at room temperature for most solvent considered, and that expression (5) strongly underestimates the observed results. Indeed, detailed analysis by Chapman and Maroncelli,[5] using the expressions equivalent to (3) derived by van der Zwan and Hynes[6] for an ionic atmosphere surrounding a dipolar solute (point dipole), shows that this extended DH theory strongly underestimates (by more than an order of magnitude) the ionic contribution to the observed solvation energy even at concentrations where the theory is presumably valid.

Turning now to dynamics, the Debye and Falkenhagen (DF) theory for the relaxation of the ionic atmosphere around a central ion,[12] yields the following expression for the time-dependent charge density in the ionic atmosphere, following the onset of a point charge Q at the origin

$$\rho(r,t)=-Q\frac{\kappa^3}{8\pi\kappa r}\{\text{Erfc}[\kappa r/(2\sqrt{D\kappa^2 t})+\sqrt{D\kappa^2 t}]e^{\kappa r} + \text{Erfc}[\kappa r/(2\sqrt{D\kappa^2 t})-\sqrt{D\kappa^2 t}]e^{-\kappa r}\}, \tag{6a}$$

where D is the ions' diffusion constant (assumed for simplicity to be the same for all ions) and where

$$\text{Erfc}(x)=\frac{2}{\sqrt{\pi}}\int_x^\infty \exp(-y^2)dy=1-\text{Erf}(x). \tag{7}$$

When the central ion has a finite radius a, it can be shown (see the Appendix) that the DF solution leads to the following expression for the solvation function [Eq. (1)]:

$$S(t)=\frac{1}{1-\kappa a}\{1-\text{Erf}(\sqrt{D\kappa^2 t})-\kappa a \times\exp\{[1/(\kappa a)^2-1]D\kappa^2 t\}\text{Erfc}(\sqrt{D\kappa^2 t}/\kappa a)\}. \tag{6b}$$

Both Eqs. (6a) and (6b) decay asymptotically, for $D\kappa^2 t \gg 1$, as exponential functions of time, with the characteristic time

$$\tau_{\text{DF}}=\frac{1}{D\kappa^2}. \tag{8}$$

Alternatively, the *average* relaxation time of the ionic atmosphere can be calculated (see the Appendix), leading, for small κa, to

$$\tau_I=\int_0^\infty S(t)dt=\frac{1}{2}\tau_{\text{DF}}. \tag{9a}$$

A different result was obtained by Van der Zwan and Hynes[6] when a point dipole located in a spherical cavity of radius a was considered instead of the ion. They found for the ionic atmosphere relaxation time around the dipole τ_{ID}:

$$\tau_{ID}=\frac{a}{2D\kappa}. \tag{9b}$$

Since a^2/D is of order ~ 1 ps, we find that for $c=0.1M$ where $\kappa a \sim 0.1$ both τ_I and τ_{ID} strongly underestimate the observed relaxation times, while at higher electrolyte concentrations [e.g., $c=1M$ and $(\kappa a)\sim 1$] the discrepancy is even larger. Obviously, at such high concentrations the DF theory and its extensions break down, but we could still envision a situation where even if the ionic atmosphere does not have the characteristics of the DH distribution, the dynamics are still controlled by ion diffusion. As pointed out by Chapman and Maroncelli,[5] the rate of such a diffusion controlled process (for $c=1M$, $D=10^{-5}$ cm^2/s, and $a=1$ A) is also an order of magnitude faster than the observed rates, excluding this mechanism as the rate determining process. We note in passing that these estimates of τ_I and τ_{ID} depend on the system's static dielectric constant (which affects κ). The latter is in turn affected by the electrolyte, both because of its effect on the solvent rearrangement as well as because of the additional screening provided by ion pairs.

The discrepancy between the predictions of DH and DF based theories and between experimental observations has lead to different interpretations with regard to its origin. Huppert and co-workers[4] have suggested that the origin of this discrepancy is ion association that takes place in the relatively low permeativity solvents (as is shown by conductivity measurements) and interpreted the slow dynamics in terms of rotational diffusion of such ion pairs. Chapman and Maroncelli[5] have offered another interpretation of the solvation energy and the slow dynamics, in terms of specific ion–probe interaction and association in the first solvation layer of the probe molecule. The latter mechanism is suggested by the observed correlation between both the energetics and the dynamics of the ionic part of the solvation process and between the ions charge-to-size ratio (the dominant effect of cations is explained in this context by their smaller size), as well as by the observed temperature dependence of the dynamics, which show that the solvation is activated beyond the activation associated with the diffusion process. These observations provide strong support for the Chapman–Maroncelli interpretation,[5] even though their simple model is deficient as has been recently shown by Bart and Huppert.[4(c)] A detailed understanding of these phenomena is of utmost importance as both equilibrium solvation and solvation dynamics play major roles in determining the course and rates of chemical processes involving charge rearrangements in polar solvents.

In the present work we study charge solvation in electrolyte solutions using molecular dynamics simulations. We focus on generic aspects of this process and can therefore limit ourselves to a simple model system. We note that the experimental time scale of a few nanoseconds lies in the limits of what is feasible with "normal" computational resources. Still, we have found that in the system studied (Stockmayer solvent with relative large static dielectric constant containing dissolved structureless, i.e., spherical, ions) much of the interesting dynamics occurs on shorter time scales. In addition, these simulations enable us to focus on several important questions which could not be addressed by the experimental systems used so far, such as the effect of the electrolyte on the solvent relaxation. In this regard we note the surprising lack of salt effect on electron solvation dynamics on the sub-ps time scale, up to $11M$ electrolyte concentrations, observed by Gauduel *et al.*[13] This is in contrast to other electronic processes in solution which are affected by added salt. For example, Thompson and Simon[14] have observed a linear dependence of intersystem crossing rate in 3-amino-9-fluorenone on the square root of the ionic strength in acetonitrile/salt solutions. Finally we note that the simulations make it possible for us to observe the DF dynamics, namely to examine the buildup in time of the DH diffuse solvation layer. This is possible even though the DH solvation energy is negligibly small in the highly polar solvent that we use, because we can follow the buildup of the direct (unscreened) electrolyte–solute interaction.

The rest of this paper is constructed as follows: Section II describes our model and briefly reviews technical details of the simulation. Section III describes the simulations results with regards to the electrolyte effect on the solvent equilibrium and dynamical behavior, as well as with regard to the electrolyte dynamics itself. Section IV concludes.

II. THE SIMULATED SYSTEM

We consider a system of 700 solvent and ion particles. The solvent is a Stockmayer liquid: Lennard-Jones (LJ) particles with point dipoles at their centers. Intersolvent (two-body) interactions are thus parametrized by the Lennard-Jones parameters ε_{LJ} and σ_{LJ} $\{V_{LJ}(r)=4\varepsilon_{LJ}[\sigma_{LJ}/r)^{12}-(\sigma_{LJ}/r)^{6}]\}$ and by the magnitude of the molecular dipole μ. The solvent is also characterized by its molecular mass m, its moment of inertia I, and its density ρ_s. We have used the parameters of Neumann *et al.*,[15] given in reduced units by: $T^*=k_BT/\varepsilon_{LJ}=1.15$; $\mu^*=\mu/\sqrt{\varepsilon_{LJ}\sigma_{LJ}^3}=\sqrt{3}$; $\rho_s^*=\rho_s\sigma_{LJ}^3=0.822$; and $I^*=I/m\sigma_{LJ}^2=0.025$. The choice for ρ_s^* implies that the simulation cell edge length is $L^*=L/\sigma=9.48$. In what follows we shall often refer to the "CH_3Cl parameter set" as a particular example. This corresponds to a set of parameters chosen to mimic the properties of liquid $CH_3Cl^{3(g)}$: $\sigma_{LJ}=4.2$ Å, $\varepsilon_{LJ}=195$ K, and $m=50$ amu. This implies $T=224$ K; $\rho_s=18.4M=0.92$ g/cm^3; $\mu=2.45$ D; and $I=22.05$ amu Å^2 in the present simulation. This choice of parameters corresponds to a liquid with a high dielectric constant, $\varepsilon_s=66$. The ions are represented by LJ particles with point charges in their centers. There are equal numbers of cations and anions of the same absolute charge, and the overall system is neutral. Their absolute charge in reduced units is $q^*=q/\sqrt{\varepsilon_{LJ}\sigma_{LJ}}=6.29$ ($=0.44e$ in the "CH_3Cl" parameter set). The choice of a solvent characterized by a large static dielectric coefficient was motivated by our wish to avoid appreciable ion pairing in our system. This was indeed observed to be the case for our choices of parameters, while using considerably higher ion charges or smaller dielectric constant results in aggregation of the electrolyte.[16] The LJ parameters for the ion–ion and ion–solvent interactions were all chosen the same as those characterizing the solvent. Solvation dynamics in this system is studied by switching on, in the equilibrium solvent at time zero, an impurity ion. As in our previous simulations[3(h)] the charge of this ion was taken $Q^*=18.78$ ($Q=1.32e$). Finally, the long-range electrostatic forces were handled by using reaction field boundary conditions with the dielectric constant of the continuum surrounding the "system sphere" of radius $R_C^*=R_C/\sigma_{LJ}=L^*/2$ taken as that of the pure solvent, $\varepsilon_s=66$.

The simulations were performed at three different salt concentrations, c_I keeping the total number of ions and dipoles in the simulation cell to be 700. The numbers of salt molecules (i.e., ions of each type) in the three concentrations are 10, 35, and 100, corresponding in the CH_3Cl parameter set to the concentrations 0.26, 0.92, and $2.63M$, respectively. Because of the finite size of the simulation system it is virtually impossible to get meaningful simulations at considerably lower salt concentrations. For the same reason the results for $c_I=0.26M$ are less accurate and

less reliable than those of the higher concentrations.

In what follows we refer to the system characterized by the parameters given above and with $c_I=0.92M$ as the "standard system." Other choices of parameters and concentrations will be specified when needed.

Typical MD trajectories were obtained with the velocity Verlet algorithm, using a time step $\delta t^* = \delta t/\sqrt{(m\sigma_{LJ}^2/\epsilon_{LJ})} = 1.52\times 10^{-3}$ ($=3.5$ fs in the CH_3Cl parameter set). Equilibrium trajectories where used to obtain dielectric properties and linear response coefficients. Nonequilibrium simulations were performed to study solvation dynamics. The latter were carried out in the following way: First an equilibrium trajectory with an additional neutral impurity atom was generated. Twenty five configurations were recorded at constant time intervals of $\Delta t^*=15$. Each configuration is the starting point for two nonequilibrium trajectories: one with the impurity charge positive and one with this charge negative. This results in 50 nonequilibrium trajectories at each salt concentration. In what follows the results of these simulations are described.

III. RESULTS AND DISCUSSION

A. Equilibrium simulations

This set of simulations is performed in order to obtain equilibrium and linear response properties of the electrolyte solution. These include the dielectric constant and dielectric relaxation time, ionic mobility, and diffusion coefficients. The static dielectric constant associated with the *solvent response* ϵ_s is calculated using the fluctuation formula appropriate for the reaction field boundary conditions:[17]

$$\frac{(\epsilon_s-1)(2\epsilon_R+1)}{2\epsilon_R+\epsilon_s}=\frac{1}{kTR_C^3}\langle \mathbf{M}\cdot\mathbf{M}(R_C)\rangle, \tag{10}$$

where $R_C=L/2$ is the cut-off distance of the electrostatic potentials, L is the simulation box edge length, ϵ_R is the static dielectric constant of the continuum outside R_C which gives rise to the reaction field, $\mathbf{M}$ is the total instantaneous dipole in the simulation box, and $\mathbf{M}(R_C)$ is the total instantaneous dipole in the central sphere of radius R_C surrounding each solvent molecule (averaged over these molecules). Note that Eq. (10) should ideally yield the same result for ϵ_s for any ϵ_R. Pure solvent calculations were carried out for this system by Neumann *et al.*,[15] leading to $\epsilon_s(c_I=0)=66$. The calculation of ϵ_s for the electrolyte solution is made under the assumption that Eq. (10) (with $\mathbf{M}$ replaced by $\mathbf{M}-\langle\mathbf{M}\rangle$) remains valid also in the presence of an external field, which in the present case originates from the ions.[18] Note that ϵ_s is the dielectric response of the solvent only. One can also discuss the total dielectric response of the electrolyte solution, including the contribution of the ions,[19] however this quantity is not relevant in a description which treats the ions explicitly.

In addition, the dynamical response of the solvent is obtained from the correlation function

TABLE I. The dielectric constant and Debye relaxation time at different salt concentrations. The pure solvent properties were taken from Ref. 15. τ_D^* and τ_D(ps) represent the relaxation time in dimensionless units (defined in the text) and in ps, respectively.

	$0M$	$0.26M$	$0.92M$	$2.63M$
ϵ_S	67	63	34	16
τ_D^*	0.95	1.05	0.54	0.46
τ_D(ps)	2.2	2.5	1.3	1.07

$$\phi(t)=\frac{\langle \mathbf{M}(0)\cdot\mathbf{M}(t)\rangle}{\langle \mathbf{M}^2\rangle}. \tag{11}$$

At the two lower salt concentrations this function was found to relax exponentially, $\phi(t)=\exp(-t/\tau_\phi)$. At $c_I=2.63M$ some deviations from exponential behavior are observed, but we have nevertheless fitted the relaxation to the same exponential form. The Debye relaxation time associated with the solvent is obtained from τ_ϕ using the relation[20]

$$\tau_D=\frac{2\epsilon_R+\epsilon_s}{2\epsilon_R+1}\tau_\phi. \tag{12}$$

The results of these calculations are summarized in Table I. It is seen that the static dielectric response *associated with the solvent* decreases with increasing salt concentration. The magnitude of this effect is larger than would be implied by the decrease in the solvent concentration in these constant volume simulations. A similar trend was observed in the simulations by Caillol *et al.*,[19] in a model where the solvent is characterized by dipolar, quadropolar, and polarizability interactions and in experimental studies of electrolyte solution properties.[21] Also, the Debye relaxation becomes faster for larger salt concentrations (note that the difference between the values given for τ_D for the pure solvent system and for $c_I=0.26M$ is within the numerical error of the simulation). Experimental results[21] show a decrease of τ_D with salt concentration for associating liquids such as methanol and *N*-methyl formamide, however, the opposite effect is observed for nonassociating solvents such as acetonitrile.

The dc ($\omega=0$) diffusion properties of the ions are presented in Table II. Obviously the behaviors of the positive and negative ions in the present model are identical. This makes it easier to accumulate enough data for sufficient statistics. The tracer diffusion constant D_t is obtained by integrating the velocity autocorrelation function

TABLE II. The diffusion coefficient and the conductivity of the electrolyte solutions. The columns denoted by * are the values expressed in reduced units and those marked cgs correspond to the cgs values obtained for out standard "methyl chloride" system.

	$0.26M$		$0.92M$		$2.63M$	
	*	cgs	*	cgs	*	cgs
D_t	0.072	5.4×10^{-5}	0.063	4.8×10^{-5}	0.063	4.76×10^{-5}
D_c	0.068	5.1×10^{-5}	0.062	4.7×10^{-5}	0.063	4.76×10^{-5}

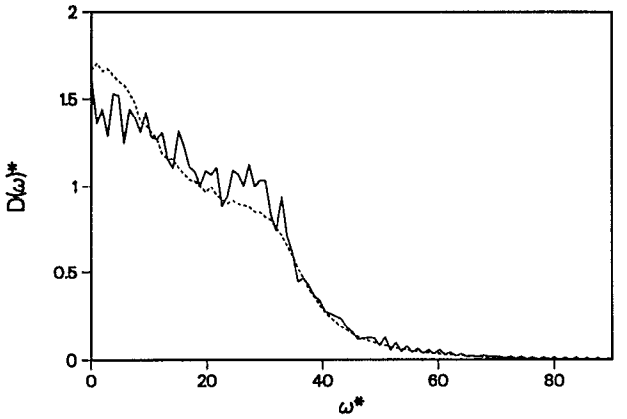

FIG. 1. The tracer (full line) and chemical (dotted line) diffusion coefficients, Eqs. (13)–(15), plotted as functions of ω for the standard system $c_I=0.92M$.

$$D_t(\omega)=\frac{1}{3}\int_0^\infty dt\, e^{i\omega t}\langle \mathbf{v}(0)\cdot\mathbf{v}(t)\rangle. \tag{13}$$

The chemical diffusion constant D_c is related to the conductivity σ via the Nernst–Einstein relation

$$D_c=\frac{k_BT\sigma}{q^2c_I} \tag{14}$$

and σ is obtained from

$$\sigma(\omega)=\frac{1}{3k_BTV}\int_0^\infty dt\, e^{i\omega t}\langle \mathbf{J}(0)\cdot\mathbf{J}(t)\rangle, \tag{15}$$

where V is the volume of the simulation cell and where $\mathbf{J}$ is the current defined in terms of the charges q_i and velocities $\mathbf{v}_i$ of the ions,

$$\mathbf{J}(t)=\sum_{i=1}^{N} q_i\mathbf{v}_i(t). \tag{16}$$

D_t and D_c are seen to be very close in all three ionic concentrations studied. This suggests that ion–ion interactions do not play a major role in our system where the solvent is highly polar. A similar observation for ionic diffusion in a solvent characterized by a relatively large dielectric coefficient was made by Caillol *et al.*[19] Note that considerable differences do exist between the frequency dependent diffusion coefficients $D_c(\omega)$ and $D_t(\omega)$ at finite frequencies, as can be seen from Fig. 1 in which both quantities are plotted as functions of ω for the standard system.

The decrease of D at higher c_I, seen in Table II, is probably associated with the increase in solvent viscosity with increasing salt concentration. This dependence is surprisingly small in our system.

The structure of the solvent and the ionic atmosphere about the charged probe is shown in Fig. 2(a), which displays, for the standard system, the pair correlation functions $g_S(r)$, $g_{IN}(r)$, and $g_{IP}(r)$ for the distributions of solvent, negative ions, and positive ions, respectively, about the probe. For definiteness we designate, here and below, ions of opposite sign to the charged solute as "negative" and those of sign similar to the solute as "positive." For the

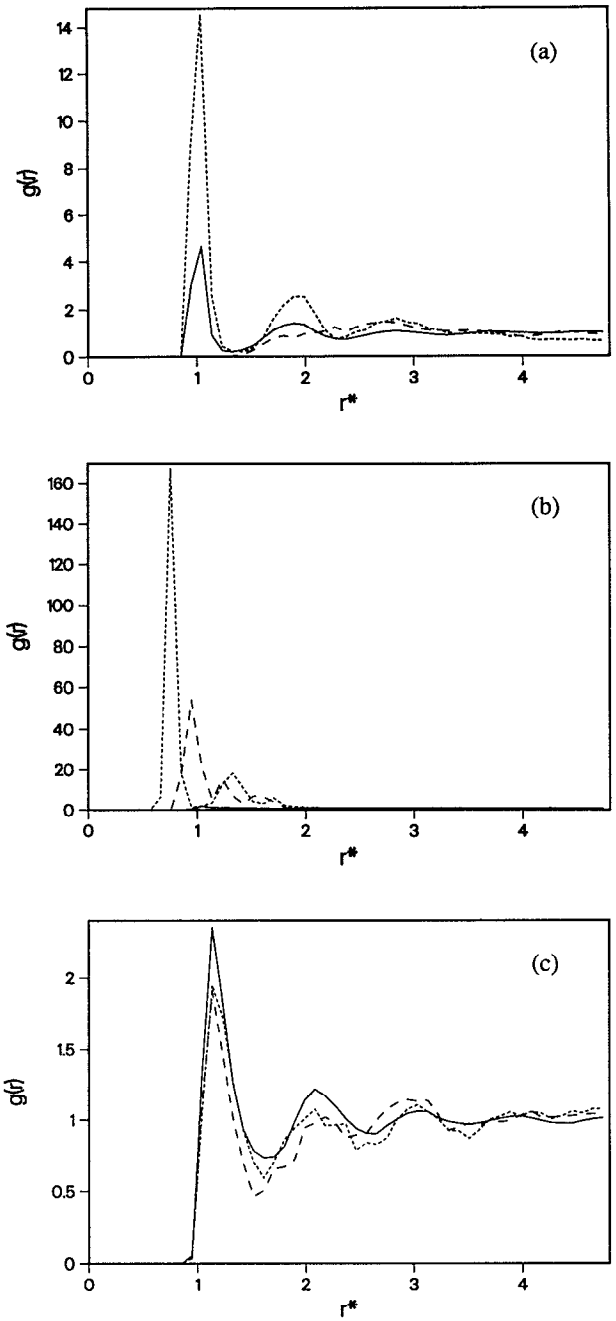

FIG. 2. The pair correlation functions $g_S(r)$ (full line), $g_{IN}(r)$ (dotted line), and $g_{IP}(r)$ (dashed line) for the distribution of solvent molecules, negative ions, and positive ions, respectively, about the (positive) solute ion. (a) Parameters of the standard system (see the text); (b) same as (a), only that the Lennard-Jones diameter of the electrolyte ions were cut in half. (c) Same parameters as in (a) only the solute is neutral.

parameters chosen there are, at equilibrium, about 1.5 negative ions and 7.5 solvent molecules in the first solvation layer surrounding the probe. This should be contrasted with the solvation structure shown in Fig. 2(b), where we use the same parameters as in Fig. 2(a) except that the LJ diameters characterizing the electrolyte ions were cut in half. The correlation functions now show a strong aggregation of negative and positive ions about the probe, resulting in solvation dominated by the ionic atmosphere. On the

TABLE III. The Debye–Falkenhagen relaxation times, Eqs. (8) and (9), and the Debye screening length, Eq. (4), at different salt concentration. The values of ε_s at each concentration are taken from Table I. Columns are marked as in Table II.

	0.26*M*		0.92*M*		2.63*M*	
	*	cgs	*	cgs	*	cgs
κ^{-1}	2.49	10.5 Å	0.976	4.10 Å	0.397	1.66 Å
τ_I	43	103 ps	7.5	18 ps	1.3	3.0 ps
τ_{ID}	8.6	20 ps	3.9	9.0 ps	1.6	3.7 ps

other extreme end, Fig. 2(c) shows the solvation structure around a neutral probe, with the same parameters as in Fig. 2(a).

The dynamics of the process that leads to these structures is discussed below. The salt concentrations used here are too high for the DH and DF theories to be valid. Nevertheless, we have used the data in Tables I and II to calculate the Debye screening length κ and the DF relaxation times τ_I [Eq. (9a)] and τ_{ID} [Eq. (9b)]. Note that in the calculation of κ we have used the dielectric response ε_s associated with the solvent in the presence of the electrolyte, as given in Table I. The results of these calculations are given in Table III.

B. Nonequilibrium simulations

In what follows we refer by "solute" or "probe" to the switched-on charge distribution. The "solvent" is the Stockmayer liquid, in which the "salt" or "electrolyte" is dissolved, giving rise to a distribution of positive and negative "ions." The solvation dynamics which follows the sudden creation or annihilation of charge on the solute is affected by both solvent and electrolyte motions. For a simple dipolar solvent, whose relaxation is dominated by rotational motion, the time scales of these contributions to the solvation process are quite different. However the simulations show that they are not independent of each other. On the contrary, at long times they are highly correlated. Indeed the bare solute–solvent and solute–ion interaction has to correlate strongly in order to give rise to the net dielectric screening of the solute–ion interactions. In particular, the DH ionic contribution to the solvation energy [Eq. (5)] contains the screening effect of the solvent. Its reduction by the factor ε_s must involve, simultaneously with the ionic atmosphere relaxation, a solvent motion and a corresponding change in the solvent–solute interaction. This is not taken into account in Eq. (3), where the term in square brackets, which correspond to the solvent, is not affected by the presence of the ions.

Consider first the solvent relaxation. As discussed in the Introduction, it can be divided into the inertial regime which is characterized by a Gaussian relaxation, and a diffusional regime where, for the pure solvent, the relaxation can be fitted to an exponential, see Eq. (2) and Refs. 3(g) and 3(i). Figure 3 shows the solvent contribution to the electrostatic part of the solvation energy $[\frac{1}{2}Q\Phi_s(t)$ where $\Phi_s(t)$ is the solvent electrostatic potential at the solute's position] for the standard system. Shown are the

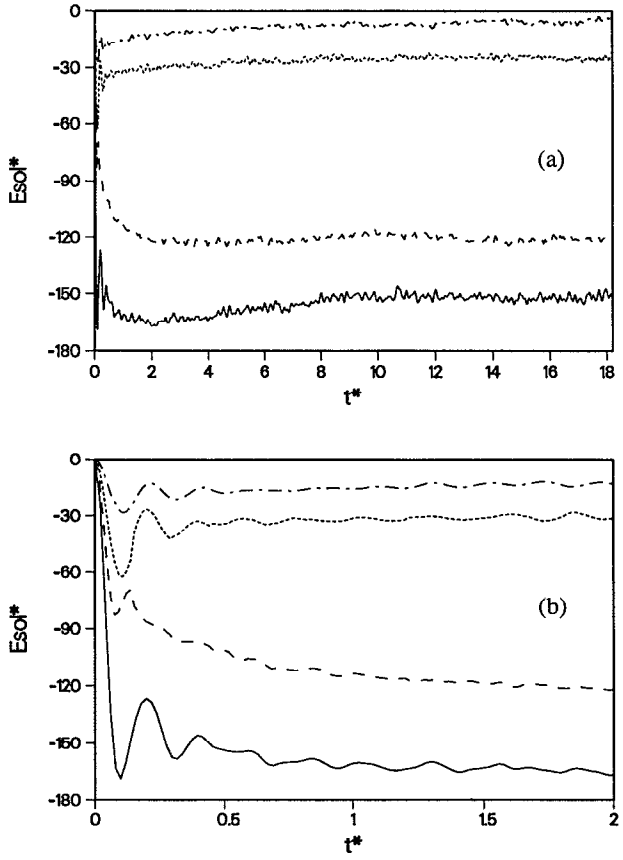

FIG. 3. (a) The solvent contribution to the solvation energy at early time. Full line—total solvation energy. Dashed line—contribution of solvent molecules in the first solvation layer. Dotted line—contribution of the second solvation layer. Dashed–dotted line contribution of the rest of the solvent in the simulation cell. (b) An expanded short-time section of the same results.

total solvent contribution and the contributions associated with the three solvation layers defined by the ion–solvent pair distribution function in the final equilibrium state [Fig. 2(a)].[22]

It is seen that the solvent relaxation can be roughly divided into three regimes: The inertial Gaussian regime is very similar to the equivalent regime in the pure solvent case.[3(g),3(i)] The subsequent diffusional relaxation now merges into a regime that was absent in the pure solvent. In this latter regime the solvent–solute interaction *decreases* as ions move in, forcing solvent molecules out of the immediate vicinity of the solute.

Consider now the dynamics associated with the ionic atmosphere. The (bare) electrolyte contribution to the solvation energy $[\frac{1}{2}Q\Phi_I(t)$ where $\Phi_I(t)$ is the electrostatic potential due to the ions at the solute's position] is shown as a function of time, for the standard system, in Fig. 4. It is seen that the overall ionic response is mostly exponential, with a small initial Gaussian component. It is of interest to compare the different behaviors of positive and negative salt ions during the formation of the ionic atmosphere. Figure 5 shows these relaxation processes following the onset of the solute charge in the standard system. The results for the other salt concentrations are qualitatively

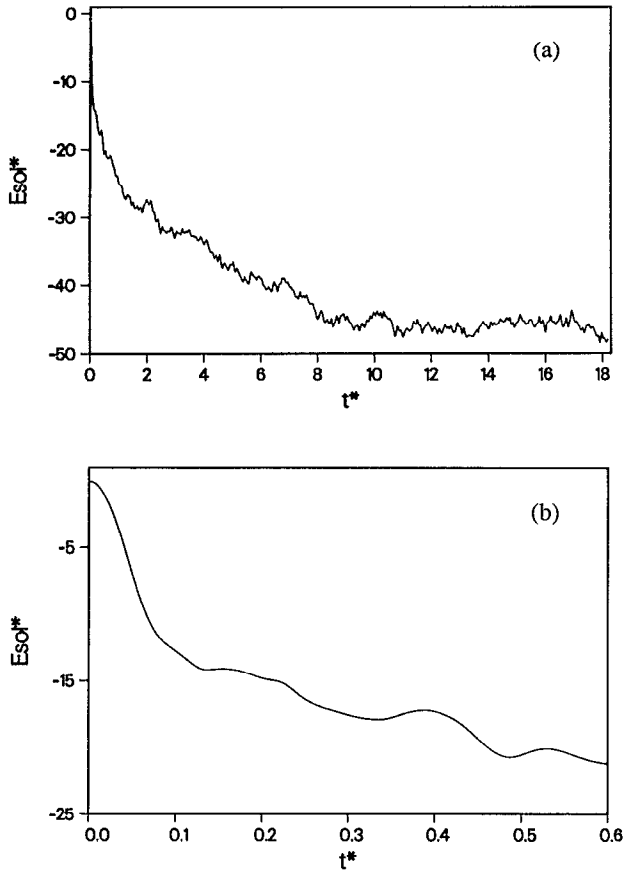

FIG. 4. (a) The ionic contribution to the solvation energy at early times. (b) An expanded short-time section of (a).

similar. Since the mobilities of the two ion types are the same, the two time evolutions would be identical in the DH–DF limit. The large differences between the relaxation processes seen in Fig. 5 is a clear demonstration of the breakdown of these linear theories.[23] Following the switching on of the solute charge, positive ions move quickly (on a time scale <1 in reduced units, ~ 2 ps in the CH_3Cl

FIG. 5. Positive ion (full line) and negative ion (dotted line) contributions to the solvation energy of the (positive) probe solute, following the onset of the solute charge in the standard system. For clarity, the negative ion line is shifted to the same energy origin as the positive ion line.

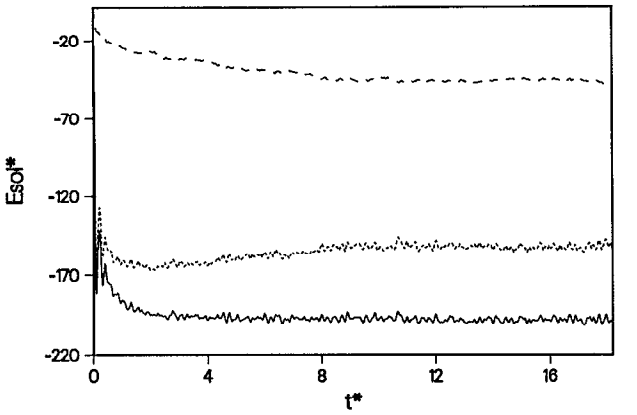

FIG. 6. The early time evolution of the total solvation energy (full line), the solvent contribution (dotted line), and ionic contribution (dashed line) following the onset, at $t=0$, of the solute charge in the standard system.

parameter set) out of the first solvation layer. Once out, their residual interaction with the solute is small and changes slowly. Negative ions on the other hand start more slowly as they move in from the second solvation layer, but they continue to come in at longer time and eventually contribute more to the ionic part of the solvation energy. A similar observation was recently made by Knödler and Dietrich[24] in lattice simulation of ionic relaxation about a charged probe.

The early time evolution of the total solvation energy for the standard system is displayed together with its solvent and salt components in Fig. 6. The total solvation energy, represented by the full line in Fig. 6, is seen to relax quickly for this system, and reaches its final equilibrium value at $t^* \cong 4$. A slower time scale is seen in the individual solvent and ions components. The solvent contribution to the solvation energy [dotted line, identical to the full line of Fig. 3(a)] decreases (becomes less negative) on this slow time scale as the solvent responds to the slow creation of the ionic atmosphere about the charged solute. The absence of a net effect on the total solvation energy on this longer time scale amounts to an almost complete screening of the ion–solute interaction by the solvent. This is particularly noteworthy, because the interaction of the charged solute with an ion at contact is, for the present choice of parameters, almost four times stronger than the contact interaction of the same solute with a fully oriented solvent dipole (by "contact" we mean that the distance between centers is equal to the arithmetic average of the corresponding LJ diameters). However, this screening cannot be accounted for fully by macroscopic electrostatics because as seen above (Fig. 2), between one and two ions reside in the first solvation shell of the solute in equilibrium. The observation that the time scales associated with the individual, solvent, and ions', contributions to the total solvation energy are different from the time scale associated with their sum is discussed again below.

The full time scale displayed in Fig. 6 (18 reduced units $=42$ ps in the CH_3Cl parameter set) is short relative

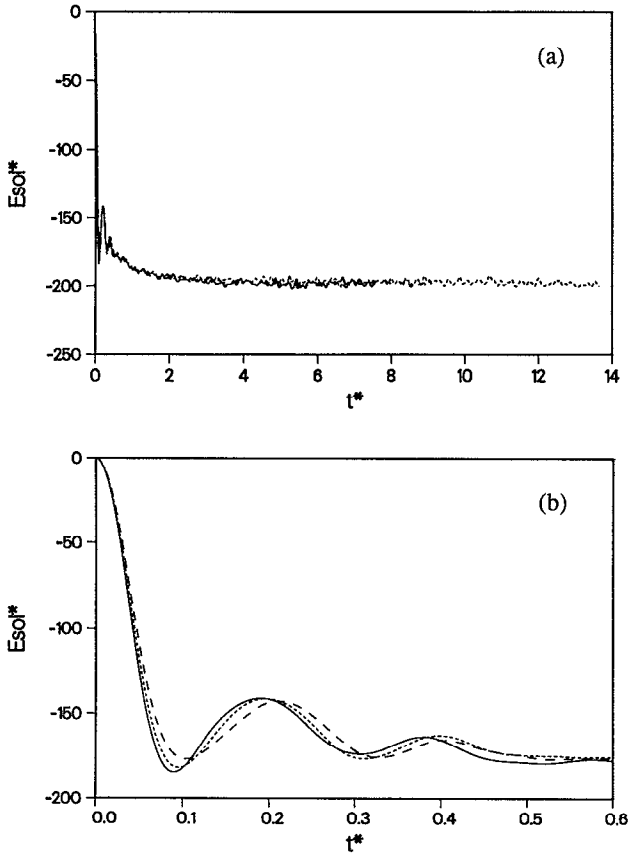

FIG. 7. (a) The time evolution of the total solvation energy at the three salt concentrations: Full line: $c_1=0.26M$. Dotted line: $c_I=0.92M$. Dashed line: $c_I=2.63M$. (b) An expanded short-time section of (a).

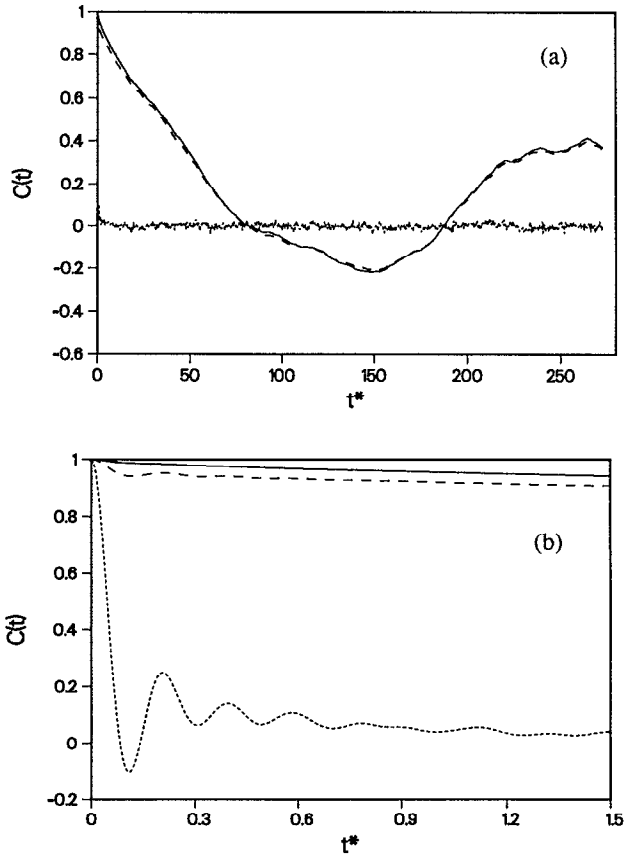

FIG. 8. (a) The correlation function $C(t)$ (dotted line), $C_S(t)$ (dashed line), and $C_I(t)$ (full line) obtained from a single long (820 reduced time units) equilibrium trajectory for the standard system containing a charged solute. (b) An expanded short-time section of (a).

to those observed experimentally. Indeed, the solvation structure about the probe has not yet reached equilibrium as is evidenced by the fact that the individual solvent and ions' components of the solvation energy are far from their average equilibrium values (see discussion of Fig. 11 below). The average number of negative ions in the first solvation shell around the positive solute at the end of the 50 runs whose combined output is displayed in Fig. 6 is ~ 0.8 while in equilibrium this number is ~ 1.5. It is remarkable that the residual slow time evolution is taking place while the total solvation energy remains almost constant (for the present system), practically at its final equilibrium value.

This almost complete screening of the ions' potential by the solvent which is seen to take place in our standard system results in the absence of salt effect on the total solvation energy and on its time evolution in this system, as seen in Fig. 7. Figure 7(a) shows the total solvation energy as a function of time for the three salt concentrations. An expanded section of the corresponding initial decay is shown in Fig. 7(b). Both the inertial Gaussian relaxation observed on the fast time scale and the consecutive exponential relaxation with superimposed inertial oscillations are seen to be practically independent of the salt concentration in the range studied. The Gaussian time inferred from Fig. 8(b) is, within numerical noise, the same as in the pure solvent. This is also true for the overall solvation energy. The latter observation is reminiscent of the absence of salt effect on the solvation red shift in highly polar solvents such as water and formamide.[4,5] Obviously, for other choices of parameters, e.g., ions charges and sizes, the individual solvent and ions' contributions to the solvation energy will not fully compensate each other, leading to an overall salt effect on the solvation energetics and dynamics, as seen below.

The dependence of several quantities which characterize the time evolution of the solvation on the salt concen-

TABLE IV. The results of a fit of the initial part of the total solvation energy, from the nonequilibrium simulations, to a Gaussian with a time constant τ_g^* and of the initial solvent contribution to a Gaussian with a time constant τ_{gS}^*. Also presented is a fit of the ionic contribution to the function given in Eq. (17).

	$0.26M$	$0.92M$	$2.63M$
τ_g^*	0.066	0.066	0.064
τ_{gS}^*	0.066	0.066	0.062
τ_{gI}^*	0.081	0.088	0.082
A_{gI}^*	4.63	17	51
τ_{eI}^*		4.21	2.31
A_{eI}^*		31	42

tration is shown in Table IV. Given are the Gaussian times τ_g associated with the total solvation energy, and the Gaussian times τ_{gI} and τ_{gS} associated with the separate electrolyte and solvent contributions, respectively, to this quantity. Also given for the two higher salt concentration quantities A_{gI}, are A_{eI} and τ_{eI} obtained by fitting the short-time evolution[25] of the electrolyte contribution to the solvation energy (Fig. 4), to the function

$$W_{sI}(t) = -(A_{gI}+A_{eI}) + A_{gI}e^{-(t/\tau_{gI})^2} + A_{eI}e^{-t/\tau_{eI}}. \tag{17}$$

The following points should be noticed:

(a) The Gaussian time constant τ_g, which accounts for much of the total solvation energy, is equal, within the computational noise, to the solvent Gaussian time τ_{gS}, and shows practically no or very little dependence on the salt concentration in the range studied. Within the computational error this time is identical to that obtained for the pure solvent. Also, the inertial time τ_{gI} associated with the (unscreened) electrolyte contribution depends only weakly, if at all, on the salt concentration, and is remarkably similar to τ_{gS}.

(b) The exponential time τ_{eI} depends strongly on the electrolyte concentration and decreases when the electrolyte concentration increases.

(c) The times τ_{eI} which, except for the small Gaussian component, correspond to the *early time evolution* of the ionic atmosphere about the solute, are of the same order of magnitude as those estimated from the average time τ_I, Eq. (9a), associated with the linear DF theory. This observation is based on the two higher salt concentrations for which τ_{eI} could be determined from the simulations.[25] Note that our nonequilibrium simulation were not long enough to distinguish the corresponding time ($\tau_I=43$ in reduced units) in the low concentration case. It should be kept in mind that the DH and the DF theories are invalid at the concentrations considered in the present simulations, however, it appears that this intermediate dynamics probes a similar process, namely ions diffusion toward and away from the solute center. Also, we should emphasize that in view of our limited statistical averaging, the *quantitative* aspects of the observations described above should be regarded only as rough estimates.

(d) As discussed above, the time evolution of the electrolyte motion near the solute has a considerably slower regime which cannot be probed by our relatively short nonequilibrium simulations. We have inferred the existence of this slower time scale from the fact that the separate ionic and solvent contributions to the solvation energy did not reach their equilibrium values on the time scale of our nonequilibrium simulations.

(e) There have recently been several studies[8] of the nature of the inertial part of the relaxation, characterized by the Gaussian time evolution seen in Figs. 3(b) and 7(b). Within linear response theory the short-time evolution of the solvation function $S(t)$ may be shown[26] to be given by $S(t) \sim e^{-(t/\tau_g)^2}$ where

$$\tau_g^2 = 2\frac{\langle\delta\Phi^2\rangle}{\langle\delta\dot{\Phi}^2\rangle}, \tag{18}$$

where $\Phi(t)$ is the potential induced by the solution (solvent and ions) at the position of the solute at time t, and where $\delta\Phi$ represents the fluctuation of this quantity from its equilibrium value. If we assume that the motions that contribute primarily are the rotational motions of the solvent dipoles and the translational motions of the ions, the denominator in Eq. (18) takes the form[8(c)]

$$\langle\delta\dot{\Phi}^2\rangle = \frac{2k_BT}{3I}\mu^2\sum_j\langle r_j^{-4}\rangle + \frac{k_BT}{m}q^2\sum_i\langle r_i^{-4}\rangle, \tag{19}$$

where the sum over j goes over solvent molecules of dipole moment μ and moment of inertia I, while the other sum goes over ions of charge q and mass m. The denominator of Eq. (18) is obtained, within linear response theory, from the relation $\langle\delta\Phi^2\rangle = -k_BT(\partial\langle\Phi\rangle/\partial Q)$ where $\langle\Phi\rangle$ is the electrostatic potential at the solute, given in the DH theory by

$$\langle\Phi\rangle = -\frac{Q}{a}\left[\frac{1}{\varepsilon_s}\frac{\kappa a}{1+\kappa a} + \left(1-\frac{1}{\varepsilon_s}\right)\right]. \tag{20}$$

If $\varepsilon_s \gg 1$ this gives $\langle\Phi\rangle \cong -(Q/a)$, so $\langle\delta\Phi^2\rangle = k_BT/a$. This leads to

$$\tau_g^{-2} = \frac{a}{3I}\mu^2\sum_j\langle r_j^{-4}\rangle + \frac{a}{2m}q^2\sum_i\langle r_i^{-4}\rangle. \tag{21}$$

Note that even though τ_g^{-2} appears to consist of separate contributions associated with the solvent and the electrolyte, we cannot write equations similar to Eq. (21) for the individual times τ_{gS} and τ_{gI}. It appears that, both from experimental and theoretical points of view, only τ_g is a meaningful quantity even though τ_{gS} and τ_{gI} could be estimated from the simulation results.

Using the parameters given in Sec. II, Eq. (21) yields $\tau_g^* = 0.0492$, 0.0495, 0.0505, and 0.0531 for the systems with salt concentrations 0, 0.26, 0.92, and 2.63M, respectively. These times are all within less than 10% of each other and are about 10% shorter than the estimates based on linear response simulations [e.g., Fig. 8(b) below]. Note however that while Eq. (21) can rationalize the observed insensitivity of τ_g to salt concentration, it underestimates by about 20% the observed Gaussian times obtained from the nonequilibrium simulations (Table IV).

More insight into the nature of the relaxation dynamics may be obtained by considering the dynamics of equilibrium fluctuations. Recall that for solvation dynamics in pure dielectric solvents equilibrium correlation functions give a good approximation to the nonequilibrium solvation [e.g., $S(t) \cong C(t) \equiv \langle\delta\Phi(0)\delta\Phi(t)\rangle/\langle\delta\Phi^2\rangle$].[3(a),3(d),3(e),3(g),3(i)] It makes relatively little difference whether $C(t)$ is calculated in the initial uncharged solute or the final charged equilibrium state. Here we expect considerably larger differences because the solvation structure about the solute is very different in the two states.

Figure 8 shows the time evolution of the correlation function $C(t)$ obtained from an equilibrium trajectory for the standard system containing a charged solute. Also

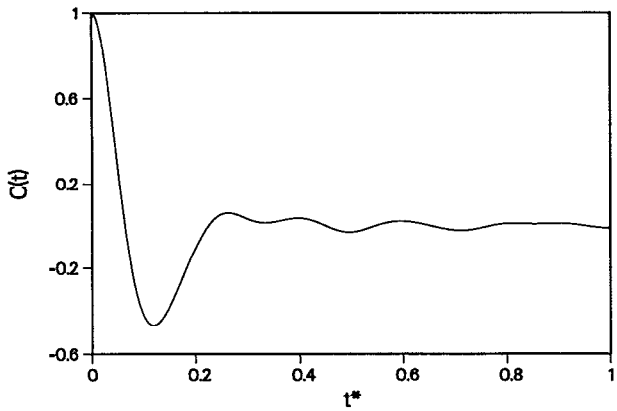

FIG. 9. The course grained correlation function $\tilde{C}_S(t)$ (see the text) for the standard system.

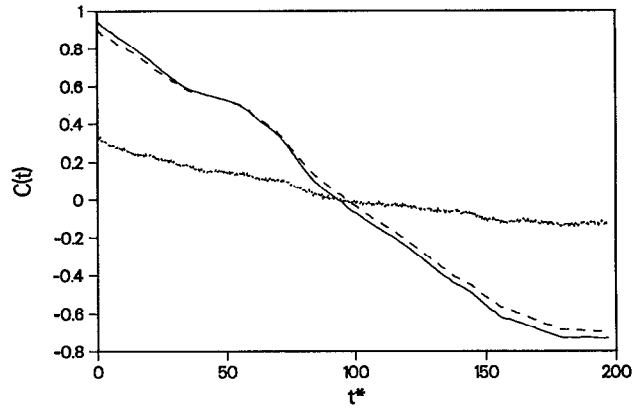

FIG. 10. Same as Fig. 8, for parameters similar to those characterizing the standard system except that the LJ diameter of the salt ions are smaller by a factor of 2.

shown are the correlation functions associated with the solvent and ions separately [i.e., $C_S(t) \equiv \langle \delta\Phi_S(0)\delta\Phi_S(t)\rangle / \langle \delta\Phi_S^2\rangle$ for the solvent and $C_I(t) \equiv \langle \delta\Phi_I(0)\delta\Phi_I(t)\rangle / \langle \delta\Phi_I^2\rangle$ for the ions, where $\delta\Phi_S(t)$ and $\delta\Phi_I(t)$ are the fluctuations of the potentials due to the solvent and to the ions, respectively, at the solute center, from their average values]. These functions are computed from a single long (1.91 ns) equilibrium trajectory. The function $C(t)$ shows the familiar bimodal relaxation dominated by a fast initial Gaussian evolution followed by a residual relaxation that for the present choice of parameters can be hardly observed above the thermal noise. The Gaussian time calculated for this evolution is $\tau_g^* \sim 0.056$, about midway between that reported above (0.066, cf. Table IV) for the nonequilibrium evolution and that (0.051) computed from Eq. (21). Note that the statistical error estimated for the simulated times is about 10%.

The individual contributions $C_S(t)$ and $C_I(t)$ evolve quite differently: The amplitudes of their Gaussian components are much smaller than that of $C(t)$ and their time evolutions are dominated by a long component that can be fitted to an exponential, which for the present system is characterized by a relaxation time of the order ~ 50 (reduced units). The following points should be emphasized:

(a) The fact that the solvent and the salt components of the relaxation seen in Fig. 8 show the same long-time behavior is associated with the fact that this motion is dominated by the salt, with the solvent dipoles following essentially adiabatically, so as to screen the ion–solute interactions. This screening is evident in the fact that the total correlation function $C(t)$ has reached its final value while the individual components $C_S(t)$ and $C_I(t)$ are still evolving.

(b) The time evolution of the solvent correlation function $C_S(t)$, as observed in Fig. 8, appears very different from its behavior in the pure solvent case. This difference results from the fact that only at early times ($t^* < 1$ say) this relaxation reflects the actual solvent response, while at later times the solvent motion follows that of the ions as discussed above. To emphasize this point we have plotted in Fig. 9, for the same system, the correlation function $\tilde{C}_S(t) = \langle \delta\tilde{\Phi}_S(0)\delta\tilde{\Phi}_S(t)\rangle / \langle \delta\tilde{\Phi}_S^2\rangle$ where $\tilde{\Phi}_S(t) = \Phi_S(t) - \bar{\Phi}_S(t)$ and where $\bar{\Phi}_S(t)$ is a coarse grained average, over a time interval $\Delta t^* = 1$ about t, of $\Phi_S(t)$. The slow adiabatic following evolution of the solvent is thus subtracted out in $\tilde{C}_S(t)$. Figure 9 shows that this function is indeed very similar to the solvation function in the pure solvent case.

(c) The observation that the total correlation function $C(t)$ reaches it final (zero) value on a relatively short time scale is obviously model dependent, and is related to the fact that, for the parameters that characterize our standard model, the solvent screens the electrostatic potential of the ions at the solute position very effectively. This corresponds to the experimental situations where, due to efficient screening by a highly polar solvent, the solvation energy (i.e., the experimentally observed red shift) does not depend on the salt concentration. This is true for our computer solvent as seen in Fig. 7. When this is not so, the contributions from the ions and from the solvent will not cancel, and a slow evolution of the net solvation will be observed. This is seen in Fig. 10 where the same correlation functions as in Fig. 8 are shown, for a system identical to our standard model except that the LJ diameters characterizing the salt ions where cut in half. In this case the correlation function $C(t)$ is seen to have, in addition to the initial Gaussian decay, a long-time component, with the characteristic time ~ 100–200 reduced time units (230–460 ps in the CH_3Cl parameter set). This time is much longer than the times obtained from the linear DF theory, τ_{DF} and τ_I (Table III), which demonstrates the existence of such slower time scales in these solvation processes. However, the absolute time scale associated with the relaxation cannot be determined, because, as in the previous case [Fig. 8(a)] slow fluctuations which did not average out with our statistics are seen in $C(t)$ at longer times. In addition we note that, in contrast to the previous case, strong clustering of counterions about the central ion is observed in this case [see Fig. 2(b)].

The practically complete screening characterizing the long-time behavior of the system displayed in Fig. 8 is

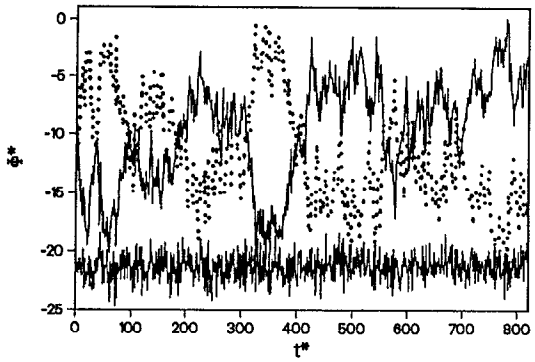

FIG. 11. The time-dependent electrostatic potential at the solute in the equilibrium standard system. Shown are the total potential $\Phi(t)$ (full lower line) and its components $\Phi_s(t)$ (dotted line), originated from the solvent and $\Phi_I(t)$ (upper full line), originated from the salt ions.

shown from another point of view in Fig. 11. Here the electrostatic potential $\Phi(t)$ at the solute, and its components $\Phi_S(t)$ and $\Phi_I(t)$ are shown as functions of time for the equilibrium standard system with a charged solute. The large, slow "screening fluctuations" in $\Phi_S(t)$ and $\Phi_I(t)$ are strongly correlated, and almost cancel in the total potential $\Phi(t)$.

Yet another view of the same dynamics is provided by Fig. 12. The full line in this figure is identical to the full (electrolyte) line in Fig. 8. The dashed and dotted curves are the correlation functions of the fluctuations from average of the *number of (negative) ions in the first solvation shell, and the sum of these numbers in the first and second solvation shells, respectively, about the charged solute.* It is seen that the linear relaxation of the solvation potential is strongly associated with, and occurs on the same time scale as the exchange of salt ions between the two solvation shells nearest to the solute, as previously suggested by Chapman and Maroncelli.[5]

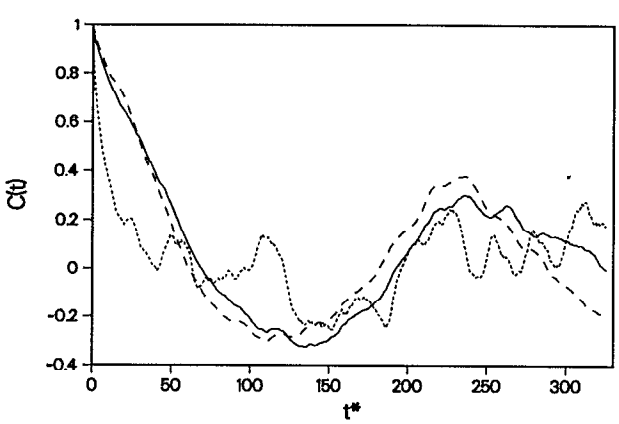

FIG. 12. Full line: the correlation function $C_I(t)$ of the electrostatic interaction $\Phi_I(t)$ between the salt ions and the solute in the standard system (identical to the full line in Fig. 8). Dashed line: the correlation function of the number of negative (opposite) ions in the first solvation layer of the solute. Dotted line: the correlation function of the number of negative ions in the first and second solvation layers about the solute.

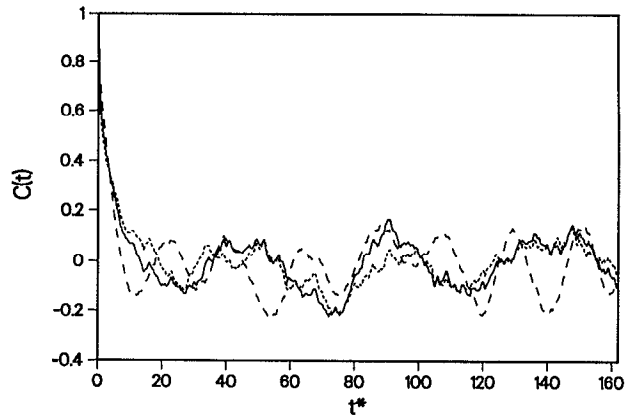

FIG. 13. The correlation function of the overall electrostatic fluctuations $C(t)$ (dotted line) as well as those from the solvent molecules $C_S(t)$ (dashed line) and from the salt ions $C_I(t)$ (full line) with a *neutral* solute.

Finally, consider the equilibrium fluctuations about a *neutral solute.* As stated above, in the case of pure solvent, we and others have found that, for solute charge of the order considered here, the correlation function $C(t)$ is not very different for the cases of charged and neutral solute. This explains the relative success of linear response theories of solvation in pure polar solvents,[8] and of numerical procedures based on such theories.[3(a),3(d),3(e),3(g),3(i)] In contrast, Fig. 13 shows that $C(t)$, as well $C_S(t)$ and $C_I(t)$ are markedly different in the neutral and in the charged solute (Fig. 8) cases. The most evident differences are (a) the faster time scale associated with the ionic motion (and the associated solvent motion) in the neutral solute case, and (b) the incomplete screening of the ions' potential at the neutral solute, which in turn gives rise to a very pronounced and relatively slow component in the relaxation of the total solvation energy inferred from this calculation. These observations can be rationalized by the following arguments:

(a) Activation energies for rearrangement of the local configuration about the solute molecule are larger in the charged solute case than for the neutral solute situation. To see this consider the activation energy for exchanging between a solvent molecule and a salt ion near the solute. This process involves a transition state where both particles are at an intermediate distance from the solute. The energy of this transition state increases with the solute charge relative to the more stable initial and final configurations. For this reason relaxation processes near the charged solute are expected to be slower than near the neutral one, as we indeed observe.

(b) Fluctuation of the *total* electrostatic potential at the solute are associated with larger fluctuations in the energy in the case of a charged solute than in the case of a neutral one. Therefore, a larger solute charge implies smaller fluctuations of this potential. Keeping in mind that $\delta\Phi=\delta\Phi_S+\delta\Phi_I$, the fact that $|\delta\Phi|$ is smaller for higher solute charge implies stronger correlations between the components $\delta\Phi_S$ and $\delta\Phi_I$ in this case. This in turn implies

that the screening effect of the solvent is less pronounced in the uncharged solute case, leading to the residual slow component observed in $\langle\Phi(t)\Phi(0)\rangle$ in this case.

IV. CONCLUSIONS

The numerical simulations described above confirm the interpretation of the slow time scale observed in the relaxation following a sudden change in solute charge distribution in electrolyte solution, as a process dominated by ion–solvent exchange in the first solvation layer about the solute. The dominance of first layer effects, as well as the high electrolyte concentrations in the system considered, make the linear Debye–Hückel (DH) and Debye–Falkenhagen (DF) theories invalid for these processes. While specific ion–probe interactions are important in the quantitative aspects of the observed solvation energy and dynamics, some general observations can be made for our generic model: (a) The short-time inertial dynamics of the solvent is only weakly sensitive to the added salt, up to several molar concentration. (b) Following the initial fast relaxation of the solvent, a slower evolution determined by ion motion and solvent adiabatic following takes place. On this time scale the solvent–solute interaction energy goes down as the counterions move in, replacing solvent molecules. (c) The relaxation of the ionic atmosphere is dominated on the short time scale by a DF-like process (ion diffusion in the solute field) and on longer time scale by the (probably activated) process of counterions transition into the first solvation layer of the solute. (d) The time evolution of the densities and hence of the corresponding contributions to the solvation energy of positive and negative ions is different, in marked deviation from the predictions of the DH and DF theories. (e) The magnitude of the solvation energy and its time evolution is not sensitive to the salt concentration in the highly polar solvent ($\varepsilon_s=66$) considered here. (f) The individual (ions and solvent) contributions to the total solvation energy are dominated by a slow component (hundreds of picoseconds) associated with solute solvent exchange in the first solvation layer about the solute. The appearance of this component in the overall solvation energy depends on the specific ion–solute and solvent–solute interactions. (g) The equilibrium fluctuations in the individual ion–solute and solvent–solute interactions are much larger than the fluctuations in the overall solvation energy. These fluctuations are strongly correlated. The correlations increase and the fluctuations in the total electrostatic potential at the solute decrease with increasing solute charge. Also, the characteristic times of these fluctuations become longer with increasing solute charge, due to the larger activation barrier for the ion–solvent exchange process. (h) The latter observation implies that linear response to a charged solute is markedly different from linear response about a neutral solute, in contrast to the observation made in most simulations of pure dielectric solvents.

Finally these observations imply that the effect of added salt on the dynamics of chemical reactions involving charge rearrangement in dielectric solvents may be quite different from that predicted in earlier theories,[6] which relied on generalizations of the Debye–Falkenhagen theory. This issue deserves further work.

ACKNOWLEDGMENTS

This research was supported by the Israel Science Foundation and by the U.S.A.–Israel Binational Science Foundation. We thank Professor D. Huppert for suggesting the problem and for many useful discussions and Professor M. Berkowitz, Professor W. Dietrich, Professor M. Ratner, and D. Knödler for many helpful discussions.

APPENDIX: THE IONIC ATMOSPHERE SOLVATION FUNCTION

This Appendix describes a derivation of the solvation function $S(t)$ defined in Eq. (1), of a spherical ionic solute of radius a, immersed in an electrolyte solution. Only the ionic atmosphere response is considered, assuming the solvent response to be much faster. The derivation use the dynamic equation for the charge density $\rho(r,t)$ developed by Debye and Falkenhagen.[12] These equations are valid for very low salt concentrations.

Under linear response assumptions the solvation energy $E(t)$ is given by

$$E(t)=\tfrac{1}{2}Q\phi(|\mathbf{r}|=a,t). \tag{A1}$$

$\phi(|\mathbf{r}|=a,t)$ is the electrostatic potential at the solute surface at time t (the origin is chosen at the solute center). Therefore, in order to determine the solvation energy, the Poisson equation for the electrostatic potential has to be solved:

$$\nabla^2\phi(\mathbf{r},t)=-\frac{4\pi}{\varepsilon_s}\rho(\mathbf{r},t). \tag{A2}$$

Since the system is spherical symmetric the solution can be given in terms of the distance from the origin r. The solution to the Poisson equation is divided into two regions, $\phi_{\text{in}}(r,t)$ for $r<a$ and $\phi_{\text{out}}(r,t)$ for $r\geqslant a$. The boundary conditions are determined from the continuity of the electrostatic potential and of the electric field at $r=a$,

$$\phi_{\text{in}}(r=a,t)=\phi_{\text{out}}(r=a,t), \tag{A3a}$$

$$\frac{\partial}{\partial r}\phi_{\text{in}}(r=a,t)=\varepsilon_s\frac{\partial}{\partial r}\phi_{\text{out}}(r=a,t). \tag{A3b}$$

The potential inside the solute cavity is immediately obtained in the form

$$\phi_{\text{in}}(r,t)=\frac{Q}{r}+B(t). \tag{A4}$$

While the boundary condition (A3a) does not give new information on $\phi_{\text{out}}(r,t)$, the boundary condition (A3b), using Eq. (A4), gives

$$\frac{\partial}{\partial r}\phi_{\text{out}}(r=a,t)=\frac{-Q}{\varepsilon_s a^2}. \tag{A5}$$

In order to solve the Poisson equation, Eq. (A2), the time-dependent charge density $\rho(\mathbf{r},t)$ has to be known. In

order to determine $\rho(\mathbf{r},t)$ the DF theory is employed. Debye and Falkenhagen derived the following diffusion equation for $\rho(\mathbf{r},t)$ in the limit of very low salt concentration:

$$\dot{\rho}(\mathbf{r},t)=D\left[\nabla^2\rho(\mathbf{r},t)+\frac{\varepsilon_s\kappa^2}{4\pi}\nabla^2\phi(\mathbf{r},t)\right]. \tag{A6}$$

Since the ions cannot penetrate the solute cavity, there is no ionic flux at $r=a$ tangent to the surface of the sphere. This is expressed by the following boundary condition:

$$\frac{\partial\rho(r=a,t)}{\partial r}+\frac{\varepsilon_s\kappa^2}{4\pi}\frac{\partial\phi(r=a,t)}{\partial r}=0. \tag{A7}$$

It is useful to make a Laplace transformation of the DF equation, Eq. (A6), using the initial condition $\rho(\mathbf{r},0)=0$ (the solute charge is switched on at $t=0$), and of the Poisson equation, Eq. (A2):

$$\nabla^2\tilde{\rho}(\mathbf{r},p)=K^2(p)\tilde{\rho}(\mathbf{r},p), \tag{A8a}$$

$$\nabla^2\tilde{\phi}(\mathbf{r},p)=\frac{-4\pi}{\varepsilon_s}\tilde{\rho}(\mathbf{r},p), \tag{A8b}$$

where $\tilde{\rho}(\mathbf{r},p)$ and $\tilde{\phi}(\mathbf{r},p)$ are the Laplace transforms of $\rho(\mathbf{r},t)$ and $\phi(\mathbf{r},t)$, respectively. $K(p)$ is defined by the relation

$$K^2(p)=\kappa^2(1+p/D\kappa^2). \tag{A9}$$

The solution to the coupled equations (A8), taking into account the boundary conditions (A5) and (A7), is

$$\tilde{\phi}_{\text{out}}(\mathbf{r},p)=\frac{Q}{\varepsilon r DK^2(p)}+\frac{Q\kappa^2e^{K(p)(r-a)}}{\varepsilon rK^2(p)[1+K(p)a]p}. \tag{A10}$$

The potential at $r=a$ after inverse Laplace transformation of Eq. (A10):

$$\phi(a,t)=\frac{Q}{\varepsilon_s a}\frac{1}{1-(\kappa a)^2}\{1-\kappa a\,\text{Erf}(\sqrt{D\kappa^2t})-(\kappa a)^2 \times\exp\{[1/(\kappa a)^2-1]D\kappa^2t\}\text{Erfc}(\sqrt{D\kappa^2t}/\kappa a)\} \tag{A11}$$

and the solvation function $S(t)$:

$$S(t)=\frac{1}{1-\kappa a}\{1-\text{Erf}(\sqrt{D\kappa^2t})-\kappa a \times\exp\{[1/(\kappa a)^2-1]D\kappa^2t\}\text{Erfc}(\sqrt{D\kappa^2t}/\kappa a)\}. \tag{A12}$$

The solvation time τ_I is readily obtained from the Laplace transform of the solvation function

$$\tau_I=\int_0^\infty S(t)dt=\tilde{S}(0)=\frac{1+2\kappa a}{2+2\kappa a}\tau_{\text{DF}}, \tag{A13}$$

where τ_{DF} is given in Eq. (8). For $\kappa a\ll 1$,

$$\tau_I=\tfrac{1}{2}\tau_{\text{DF}}. \tag{A14}$$

The asymptotic behavior of $S(t)$, at $t\gg\tau_{\text{DF}}$, is given by

$$S(t)\sim(t/\tau_{\text{DF}})^{-1/2}e^{-(t/\tau_{\text{DF}})}. \tag{A15}$$

[1] W. Jarzeba, G. C. Walker, A. E. Johnson, and P. F. Barbara, Chem. Phys. **152**, 57 (1991), and references therein.

[2] (a) P. G. Wolynes, J. Chem. Phys. **86**, 5133 (1987); (b) I. Rips, J. Klafter, and J. Jortner, *ibid.* **88**, 2346 (1988); (c) A. L. Nichols III and P. G. Wolynes, *ibid.* **89**, 3783 (1991); (d) D. F. Calef and P. G. Wolynes, *ibid.* **78**, 4145 (1983); (e) B. Bagchi and A. Chandra, Adv. Chem. Phys. **80**, 1 (1991), and references therein; (f) L. E. Fried and S. Mukamel, J. Chem. Phys. **93**, 932 (1990); (g) F. O. Ranieri, Y. Zhou, H. L. Friedman, and G. Stell, Chem. Phys. **152**, 201 (1991).

[3] (a) M. Maroncelli and G. R. Fleming, J. Chem. Phys. **89**, 5044 (1988); (b) R. N. Barnett, U. Landman, and A. Nitzan, *ibid.* **90**, 4413 (1990); (c) P. J. Rossky and J. Schnitker, J. Phys. Chem. **92**, 4277 (1989); (d) M. Maroncelli, J. Chem. Phys. **94**, 2084 (1991); (e) E. A. Carter and J. T. Hynes, *ibid.* **94**, 5961 (1991); (f) T. Fonseca and B. M. Ladanyi, J. Phys. Chem. **95**, 2116 (1991); (g) E. Neria and A. Nitzan, J. Chem. Phys. **96**, 5433 (1992); (h) E. Neria, A. Nitzan, R. N. Barnett, and U. Landman, *Proceedings of UPS*, edited by A. Laubereau and A. Seilmeier (IOP, Bristol, 1991); (i) L. Perera and M. Berkowitz, J. Chem. Phys. **96**, 3032 (1992).

[4] (a) D. Huppert and V. Itah, in *Perspectives in Photosynthesis*, edited by J. Jortner and B. Pullman (Kluwer, Dordrecht, 1990), pp. 301–316; (b) V. Itah and D. Huppert, Chem. Phys. Lett. **173**, 496 (1990); (c) E. Bart and D. Huppert, *ibid.* **195**, 37 (1992).

[5] C. F. Chapman and M. Maroncelli, J. Phys. Chem. **95**, 9095 (1991).

[6] G. Van der Zwan and J. T. Hynes, Chem. Phys. **152**, 169 (1991).

[7] S. J. Rosenthal, X. Xie, M. Du, and G. R. Fleming, J. Chem. Phys. **94**, 4715 (1991); M. Cho, S. J. Rosenthal, N. F. Scherer, L. D. Ziegler, and G. R. Fleming, *ibid.* **96**, 5033 (1992); M. Maroncelli, P. V. Kumar, A. Papazyan, M. L. Horng, S. J. Rosenthal, and G. R. Fleming, in *Ultrafast Dynamics and Solvent Effects*, edited by Y. Gauduel and P. J. Rossky (AIP, New York, in press).

[8] (a) A. Chandra and B. Bagchi, J. Chem. Phys. **94**, 3177 (1991); B. Bagchi and A. Chandra, *ibid.* **97**, 5126 (1992); (b) S. Roy and B. Bagchi, *ibid.* **99**, 1310 (1993); (c) M. Maroncelli, V. P. Kumar, and A. Papazyan, J. Phys. Chem. **97**, 13 (1993); A. Chandra, D. Wei, and G. N. Patey, J. Chem. Phys. (in press); (d) F. O. Raineri, H. Resat, B. C. Perng, F. Hirata, and H. L. Friedman, *ibid.* (in press); F. O. Raineri, B. C. Perng, H. L. Friedman, and F. Hirata, Chem. Phys. (in press).

[9] C. Reichardt, *Solvents and Solvent Effects in Organic Chemistry* (VCH, Weinheim, 1988).

[10] Note that what is seen is the residual diffusional part of the solvent relaxation, not the fast inertial part.

[11] R. S. Berry, S. A. Rice, and J. Ross, *Physical Chemistry* (Wiley, New York, 1980), Chap. 26.

[12] P. Debye and H. Falkenhagen, Phys. Z. **29**, 121, 401 (1928).

[13] Y. Gauduel, S. Pommeret, A. Migus, N. Yamada, and A. Antonetti, J. Am. Chem. Soc. **112**, 2925 (1990).

[14] P. A. Thompson and J. D. Simon, J. Chem. Phys. **97**, 4792 (1992).

[15] M. Neumann, O. Steinhauser, and G. S. Pawley, Mol. Phys. **52**, 97 (1984).

[16] M. Forsyth, V. A. Payne, M. A. Ratner, S. W. de Leeuw, and D. F. Shriver, Solid State Ion. **53–56**, 1011 (1992).

[17] S. W. de Leeuw, J. W. Perram, and E. R. Smith, Annu. Rev. Phys. Chem. **37**, 245 (1986).

[18] A similar assumption was made by Caillol *et al.* (Ref. 19) in the same context. However, these authors used a different, more restricted, procedure to calculate ε_s. Note that for a homogeneous distribution of ions $\langle M\rangle=0$.

[19] J. M. Caillol, D. Levesque, and J. J. Weis, J. Chem. Phys. **85**, 6645 (1986); **91**, 5544 (1989); **91**, 5555 (1989).

[20] M. Neumann and O. Steinhauser, Chem. Phys. Lett. **102**, 508 (1983).

[21] J. Barthel, R. Buchner, K. Bachhuber, H. Hetzenauer, M. Kleebauer, and H. Ortmaier, Pure Appl. Chem. **62**, 2287 (1990); J. Barthel and R. Buchner, Chem. Soc. Rev. **21**, 263 (1992).

[22] From the data of Fig. 2 we define as the first solvation layer the solvent molecules up to distance $d^*=1.4$ from the solute center, second layer lies between $d^*=1.4$ and $d^*=2.3$, and the rest of the solvent lies beyond the latter distance.

[23] Another inherent deviation from the DH model is the discrete molecular nature of the simulation model. However it can be shown (Ref. 24) that the symmetry between positive and negative ions exists in the linear

limit of the lattice equivalent of the DH model.

[24] W. Dietrich and D. Knödler (unpublished results).

[25] These fits were obtained from the observed time evolution from $t^*=0$ to $t^*=18.2$ and 8.0 for $C_I=0.92$ and $2.63M$, respectively. For the low concentration, $C_I=0.26M$ simulation, the results are of lesser quality because of poorer statistics, making our fitting procedure nonconvergent in this case.

[26] (a) E. A. Carter and J. T. Hynes, J. Phys. Chem. **93**, 2184 (1989); (b) D. A. Zichi, G. Ciccotti, J. T. Hynes, and M. Ferrario, *ibid.* **93**, 6261 (1989).